Double capture cross sections in *p*-Ar collisions

H. Martinez,[1] F. B. Alarcon,[2] and A. Amaya-Tapia[1]
[1]*Instituto de Ciencias Físicas, Universidad Nacional Autónoma de México, Apartado postal 48-3, 62210, Cuernavaca, Morelos, México*
[2]*Facultad de Ciencias, Universidad Nacional Autónoma de México and Estudiante doctorado Facultad de Ciencias de la Universidad Autónoma del Estado de México, Instituto Literario 100, Col. Centro, C. P. 50000, Toluca, Estado de Mexico, Mexico*
(Received 11 July 2008; published 24 December 2008)

p-Ar collisions are investigated theoretically and experimentally at impact energies in the keV regime. Total cross sections for double electron capture of *p* on Ar are calculated by an independent-particle method in the impact energy range 3–100 keV. We have measured the absolute differential and total cross sections for double electron capture for 1.0–5.0-keV *p*-Ar collisions. The absolute differential cross section (DCS) for all the collision energies considered shows a decreasing behavior with increasing angle, exhibiting an overall decrease of three orders of magnitude. The integrated DCS is found to be between the range of 0.7×10^{-2} and 4.5×10^{-2} Å^2, displays an increasing behavior as a function of the incident energy, and merges with previous data at the high-energy side. The theoretical total cross sections reproduce the structures around 5 keV and 15 keV reported by other available measurements. The analysis of the capture into the $1s^14s^1$ hydrogen-like configuration points in the direction of a common origin for these peaks.

DOI: 10.1103/PhysRevA.78.062715 PACS number(s): 34.70.+e, 34.50.−s

I. INTRODUCTION

In the past few years an increasing attention has been devoted to inelastic processes in atomic collisions in which two or more electrons undergo a transition [1]. In the double electron capture process two electrons are transferred from one atomic system to another during the collision [2,3]. Several workers have experimentally studied this type of reactions. The cross sections for the formation of H^-, as a result of double electron capture by a proton passing through argon, have been measured experimentally for intermediate proton energies below 100 keV by Fogel *et al.* [4], Afrosimov *et al.* [5], Williams [6], and Morgan and Eriksen [7]. The wide discrepancy between the experimental values has led us to make an up-to-date experimental investigation into this problem, using the angular distribution technique as an alternative way of studying such a reaction. Although several experiments have been performed to measure the double electron capture cross section in the proton-argon collision, no reliable theoretical calculations are available for comparison with experiment. One of the main difficulties in the theoretical study of these processes resides in the description of the electron correlation interactions. For incident protons, the double capture is simplified in the sense that the incident protons have no electrons and the outgoing negative hydrogen ions exist only in their ground states. These simplifications have motivated us to calculate cross sections for double electron capture in proton-on-Ar collisions using a simple model which does not include the electron correlation interactions. In this paper we address the *p*-Ar system by angular distributions measurements between 1.0 and 5.0 keV and by means of a one-electron close-coupling two-center basis approach, which was recently applied to the *p*-Ca system [8,9] with satisfactory results for charge transfer. The two electron probabilities were calculated by statistical analysis.

II. MODEL

The reaction was modeled by a semiclassical one-electron approach for each of the outer-shell Ar electrons [9]. In a second step, the two electrons in any of the subshells that comprise the outer shell were considered in an independent two-particle model. Finally, in a third step, the sum of the four subshell contributions to the H^- cross section represents our approximation to the total channel cross section.

In the one-electron step, the nuclear motion was constrained to follow classical straight lines at constant velocity. The internuclear distance introduces the time in the description of the electronic motion by the time-dependent Schrödinger equation, in which the sum of the electron-proton and proton-nucleus Coulomb interactions plus the function centered at the Ar nucleus,

$$V(r)=\left(\frac{-1}{r_{\mathrm{Ar}}}+\frac{(-17-3r_{\mathrm{Ar}})}{r_{\mathrm{Ar}}}\exp(-2.15r_{\mathrm{Ar}})\right), \qquad (1)$$

represents the model potential. The values for the parameters in the above expression were taken from Ref. [9]. To solve the Schrödinger equation, the wave functions were expanded in the form

$$\Psi(r,t)=\sum_{i=1}^{N_{\mathrm{H}}}a_i^{\mathrm{H}}(b,t)\phi_i^{\mathrm{H}}(r_{\mathrm{H}})+\sum_{i=1}^{N_{\mathrm{Ar}}}a_i^{\mathrm{Ar}}(b,t)\phi_i^{\mathrm{Ar}}(r_{\mathrm{Ar}}), \qquad (2)$$

in which, $\Phi_i^{\mathrm{H,Ar}}$ are atomic functions centered at the corresponding nucleus and b is the impact parameter. The wave functions include translation factors. The atomic states, characterized by $i=\{n,l,m\}$, were obtained by a diagonalization of the corresponding atomic Hamiltonian in a even-tempered basis:

$$\Phi_i^{\mathrm{H,Ar}}(\vec{r})=\sum_k C_{nk}^{\mathrm{H,Ar}}\exp(-\alpha\beta^k r)r^l Y_{lm}(r), \qquad (3)$$

where the $C_{n,k}^{\mathrm{H,Ar}}$ are the largest weights obtained by the diagonalization procedure and the parameters α, β, and κ (see Table I) were determined by reproducing the atomic energy levels, shown in Table II. Special care was taken at this point, because these parameters are not unique, in the sense

TABLE I. Function parameters.

	s	*p*	*d*	*f*
α_H	0.11000	0.06100	0.042000	
β_H	1.46500	2.00000	2.00000	
κ_H	11.0000	11.00000	8.00000	
α_{Ar}	0.01004	0.02910	0.06504	0.030501
β_{Ar}	1.40916	1.30016	1.35850	1.17399
κ_{Ar}	18.00000	18.00000	16.00000	15.0000

that there are compromises in the accuracy with which some levels are reproduced, at the expense of the energy accuracy for other levels that were considered less relevant during the evolution in time of the wave functions. In the optimization procedure followed, the largest weights were assigned for $n=1-4$ in H and for $n=3-5$ in Ar. Atomic functions with positive orbital energies were included to take into account processes that compete with the H^- channel at the energy range considered, like ionization.

By projecting the wave function into the different atomic functions, the Schrödinger equation was transformed in a system of coupled equations for the expansion coefficients in Eq. (2). This system was solved numerically for internuclear distances between −100 and 100 a.u., where essentially all couplings had vanished. The classical trajectories included 232 impact parameters in the range (0.02,25), not uniformly distributed. The atomic base consists of the five *s*, four *p*, and three *d* lower states in H atom and from 3*s* to 13*s*, 3*p* to 13*p*, 3*d* to 12*d*, and 4*f* to 12*f* states in Ar. This set of functions was selected in a series of convergence tests.

In the second step, the two electron probabilities were calculated within a trinomial distribution model [10], $[P_{3lm}^{1s}+P_{3lm}^{4s}+(1-P_{3lm}^{1s}-P_{3lm}^{4s})]^2$, as the product $2P_{3lm}^{1s}P_{3lm}^{4s}$. The symbol P_{3lm}^{ns} is the probability, calculated in step 1, that an electron is transferred from the $3lm$ orbital in Ar to the *ns* level in H. The 1*s* orbital was selected because the most important contribution to the total single capture corresponds to capture in this level [9]. The 4*s* was selected because it has the closest orbital energy to one of the 3*p* states in Ar and to the ionization potential of the H^-. These two-particle probabilities are integrated over the impact parameter vector space to obtain the two-electron capture cross section contribution for electrons coming initially from the specific $3lm$ subshell in Ar. Finally the sum of these contributions yields the H^- production cross section.

III. APPARATUS AND PROCEDURE

The experimental apparatus has been described in detail elsewhere [11,12], and only a brief description will be presented here. It consists of three sections: the ion source, the scattering chamber, and the rotating section which houses the analysis and detection region. H^+ ions were produced in an arc discharge ion source containing a mixture of 75% H_2 gas (99.9% purity) and 25% Ar (99.99% purity) to enhance ion production. The ions were extracted and focused by an Einzel-type lens and directed to a Wien velocity filter in order to obtain an analyzed H^+ beam at the desired velocity. The collimated H^+ beam entered the interaction chamber, which housed a gas target cell, where the double electron capture phenomena took place to form H^-. This geometry permitted the measurement of H^- ions, the directions of which make an angle of up to $\pm 7°$ with respect to the incoming beam direction; the root-mean-square angular resolution of the system was 0.1°. The detector assembly was rotated about the center of the gas target cell so that angular distributions could be obtained. The H^- ions, separated by a 45° parabolic electrostatic analyzer, were counted by channel electron multipliers.

The measured quantities were I_0, the number of H^+ ions incident per unit area per second; *n*, the number of Ar atoms per unit volume; *L*, the effective length of the scattering

TABLE II. Orbital energies (a.u.).

	H			Ar			
n	E_s	E_p	E_d	E_s	E_p	E_d	E_f
1	−0.50000						
2	−0.12500	−0.12500					
3	−0.05555	−0.05549	−0.05556	−1.07202	−0.57797	0.05720	
4	−0.03121	−0.03023	−0.03107	−0.14237	−0.09505	−0.03200	−0.03125
5	0.00223	0.10183	−0.01786	−0.05998	−0.04552	−0.02066	−0.02000
6				−0.03304	−0.02676	−0.0143	−0.01389
7				−0.02088	−0.01759	−0.0104	−0.01020
8				−0.01429	−0.01234	−0.00210	−0.00780
9				−0.1012	−0.00890	0.02878	−0.00613
10				−0.00715	−0.00632	0.09000	−0.00480
11				−0.00494	−0.00410	0.20750	−0.00387
12				−0.00330	0.02198	0.42700	−0.00311
13				−0.00214	0.15190		
14				0.07063			

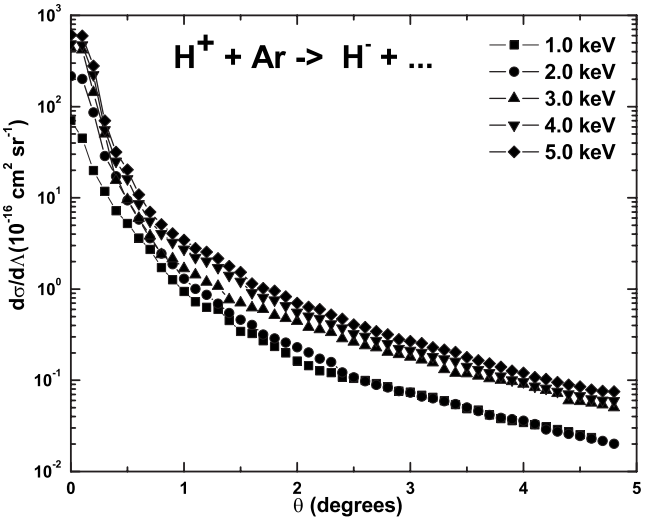

FIG. 1. Measured angular distributions for double electron capture in *p*-Ar collisions.

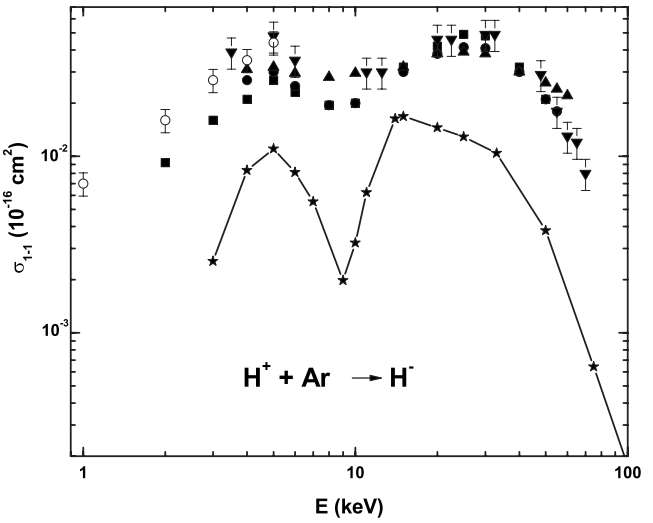

FIG. 2. Total cross sections for double electron capture in *p*-Ar collisions. Present data: (○) experiment, (★) theory, (■) from Williams [6], (▼) from Morgan and Eriksen [7], (▲) from Afrosimov [5], and (●) from Fogel [4].

chamber; and $I(\theta)$, the number of H^- ions per unit solid angle $(d\Omega)$ per second detected at angle (θ) with respect to the incident beam direction. With these measurements,

$$\frac{d\sigma}{d\Omega} = \frac{I(\theta)}{nLI_0} \tag{4}$$

was evaluated. Several angular distributions were measured on both sides of the forward direction and at different gas target pressures and $d\sigma/d\Omega$ was determined for each run. These were compared in order to assure they were symmetric and to estimate the reproducibility of the experimental results as well as to determine the limits of the "single-collision regime" since the "differential" cross section reported is absolute.

The total cross section σ for the production of H^- ions was obtained by the numerical integration of $d\sigma/d\Omega$ over all angles measured:

$$\sigma = 2\pi \int_0^{\theta_m} \frac{d\sigma}{d\Omega}. \tag{5}$$

For $\theta > \theta_m$ the differential cross sections (DCSs) vanish.

Several sources of systematic errors are present and have been discussed in previous papers [11,12]. The absolute error of the reported cross sections is believed to be less than $\pm 15\%$. This estimate accounts for both random and systematic errors.

IV. RESULTS AND DISCUSSION

Absolute DCSs data for double electron capture of H^+ ions impinging on Ar target have been measured at laboratory angles $-5.0° < \theta < 5.0°$ and collisional energies $1.0 \leqslant E \leqslant 5.0$ keV. Measurements are plotted in Fig. 1. Our measured DCSs for all collisional energies showed a decrease with increasing angle. The detected number of scattered particles at 5.0° is about three orders of magnitude smaller than those detected at zero scattering angles. Evidently this addresses our claim about the total collection of scattered particles. A vanishing cross section and background effects prevented any meaningful measurements at scattering angles higher than 5.0°, particularly at the lower collisional energies.

The differential cross sections were integrated to yield the total cross sections. The trend of these data is shown in Fig. 2, together with previous experimental data [4–7] over a wide energy range as a function of the incident energy. Error bars of $\pm 15\%$ are given to indicate the maximum reproducibility of the data in the present investigation.

Since a full analysis of the differential rate equations for tenuous target thickness needs to be corrected to second order, we have estimated the nonlinear contribution (curvature) of the curve growth [13]. We calculated the cross section taking into account the possibility of multiple collisions [13]. The value obtained for $\sigma_{1\text{-}1}$ has a maximum error of 3.5% compared to the value that we have obtained by integrating the angular distribution. The data in Figs. 1 and 2 for differential and total cross sections are corrected for multiple collisions to second order.

Figures 1 and 2 present the absolute differential and total cross section measurements for H^- production in double electron capture collisions of H^+ ions with Ar. The other above-mentioned studies employed different techniques in order to obtain total cross sections. In order to compare them with our present data for the total double electron capture of H^+ in Ar, it is imperative that uncertainties of the data reported by various groups be available. Fogel *et al.* [4] do not indicate the state of the accuracy of their data; Also, Afrosimov *et al.* [5] do not explicitly state the accuracy of their data. Williams [6] affirms that the accuracy of his cross sections is better than $\pm 25\%$; Morgan and Eriksen [7] identified the absolute error associated with their measured cross sections to be $\pm 20\%$ resulting from the absolute measurements of the target gas concentration.

The present result at 5.0 keV is in good agreement with the value obtained by Morgan and Eriksen [7], and our data

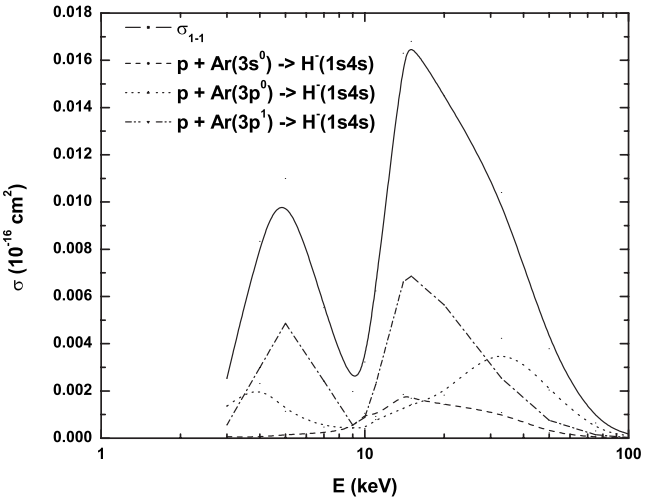

FIG. 3. Contribution to double electron capture cross sections in p-Ar collisions for electrons initially located in different subshells.

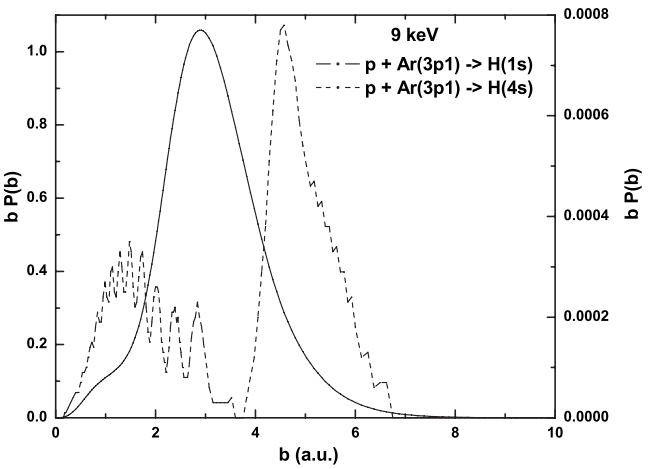

FIG. 5. Single electron capture probabilities as a function of impact parameter at collision energy of 9 keV. Left scale for capture into 1s; right scale for capture into 4s.

were found to merge smoothly into the cross sections measured by them. Both experimental results are a factor of approximately 1.5 larger than previous measurements reported. All the data follow the same behavior for the total cross section energy dependence. From Fig. 2, two maxima are evident which have approximately the same height. The theory reproduces the two peaks at around the same energy as observed in the experiments, and it shows that the peak around 15 keV is slightly higher than the one around 5 keV. This asymmetry in the height of the peaks seems to be present in the Williams-Fogel data, but not in that of Morgan and Eriksen and Afrosimov *et al.* The theoretical cross section shape is fairly similar to the experimental one. However, the theoretical results are below the experimental values by almost an order of magnitude. Since our representation of H^- is made by hydrogen like orbitals, it is not an accurate one and so we lack contributions from capture into orbitals, like the 3s. There is no way to include them in our simple model.

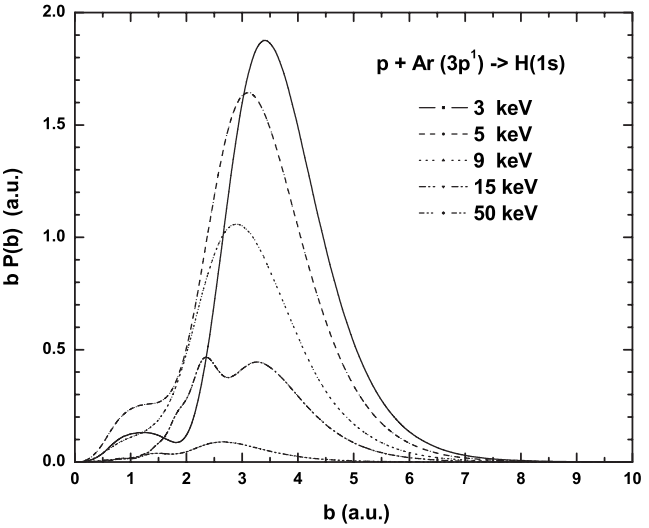

FIG. 4. Single electron capture probabilities as a function of impact parameter at collision energies of 3, 5, 9, 15, and 50 keV.

The important point is that our description reproduces the structure of the experimental measurements without invoking other channels.

What does our model says about the origin of the peaks? Figure 3 shows that the peaks at 5 keV and 15 keV are mainly produced by the contribution to the single electron capture cross sections coming from one electron that initially was in the $3p1$ or $3p-1$ energy levels. Around the minima at 3 keV and 9 keV, the contributions from all subshells are small. To understand with detail the origin of the maxima, Fig. 4 shows the weighted probabilities as a function of the impact parameter for the capture of only one electron initially at the $3p1$ subshell (which have the same value if coming from the $3p-1$ level) into the 1s hydrogen level. The corresponding curves for an electron transferred to the 4s level (not shown in the Fig. 4) are orders of magnitude smaller than those shown. It can be seen that the maxima and the areas under the curves in Fig. 4 tend to drop as the energy increases. Then, capture of only one electron into the 1s or

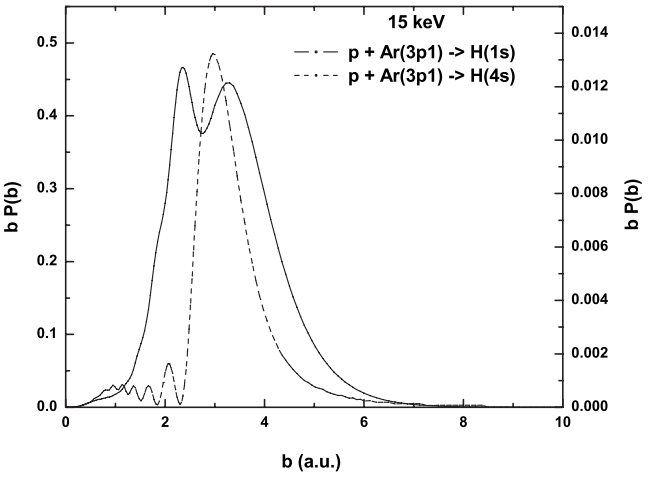

FIG. 6. Weighted single electron capture probabilities as a function of impact parameter at collision energy of 15 keV. Left scale for capture into 1s; right scale for capture into 4s.

4s cannot explain the structure appearing in Fig. 2. However, their overlap does, as shown in Figs. 5 and 6, which present the weighted probabilities as a function of the impact parameter. There is strong overlap between the main areas under the curves at 15 keV and a larger de-phasing of the corresponding areas at 9 keV. This means that the statistical model includes a dependence between the capture probabilities of one electron into the 1s level with the one for another electron into the 4s level, through the product of the probabilities. This dependence reproduces to a great extent the peaks and shape in the cross sections as a function of the incoming energy. A comparable analysis yields a similar tendency for the minimum at 3 keV and the peak at 5 keV. This result is in disagreement with the explanation given by Williams [6], indicating that the lower-energy maximum is attributed to formation of Ar^{2+} and the higher-energy maximum to formation of Ar^{3+} plus a free electron.

V. CONCLUSION

p-Ar collisions have been investigated theoretically and experimentally at impact energies in the keV regime. Total cross sections for double electron capture of p on Ar have been calculated by an independent-particle method in the impact energy range 3–100 keV. We have measured absolute differential and total cross sections for double electron capture for 1.0–5.0 keV p+Ar collisions. The absolute DCSs for all collision energies show a decreasing behavior with increasing angle, showing an overall decrease of three orders of magnitude. The total cross section is found to be between the range of 0.7×10^{-18} and 4.5×10^{-18} cm^2. The total cross sections display an increasing behavior as a function of the incident energy. Reliable previous total cross section measurements are in good agreement with those reported here. In our point of view the differences in the measured total cross sections are mainly due to different experimental techniques used by various groups. From the theoretical model it was shown that capture to the $1s^14s^1$ hydrogen-like configuration of H^- reproduces the main structures and the shape of the experimental data. These results are of fundamental interest and have potential applications in fields of aeronomy and interplanetary physics.

ACKNOWLEDGMENTS

We thank J. Rangel, A. Bustos, R. Bustos, F. Castillo, and A. Gonzalez for their technical assistance. This research was partially sponsored by DGAPA Grant No. IN-105707-3 and CONACyT Grant No. 41072-F.

[1] M. R. C. McDowell and J. P. Coleman, *Introduction to the theory of Ion-Atom Collisions* (North-Holland, Amsterdam, 1970).
[2] M. Zapukhlyak, T. Kirchner, A. Hasan, B. Tooke, and M. Schulz, Phys. Rev. A **77**, 012720 (2008).
[3] M. Schulz, T. Vajnai, and J. A. Brand, Phys. Rev. A **75**, 022717 (2007).
[4] Ia. M. Fogel, R. V. Mitin, V. F. Kozlov, and N. D. Romashko, Sov. Phys. JETP **35**, 390 (1959).
[5] V. V. Afrosimov, R. N. Il'in, and E. S. Solov'ev, Sov. Phys. Tech. Phys. **5**, 661 (1960).
[6] J. F. Williams, Phys. Rev. **150**, 7 (1966).
[7] T. J. Morgan and F. J. Eriksen, Phys. Rev. A **19**, 1448 (1979).
[8] H. Martínez and A. Amaya-Tapia, J. Phys. B **36**, 3509 (2003).
[9] A. Amaya-Tapia, H. Martinez, R. Hernández-Lamoneda, and C. D. Lin, Phys. Rev. A **62**, 052718 (2000).
[10] M. Horbatsch, Phys. Lett. A **187**, 185 (1994).
[11] H. Martinez, C. L. Hernandez, and B. J. Yousif, J. Phys. B **39**, 2535 (2006).
[12] H. Martínez and B. J. Yousif, Int. J. Mass. Spectrom. **248**, 21 (2006).
[13] E. W. McDaniel, J. B. A. Mitchell, and M. E. Rudd, *Atomic Collisions* (Wiley, New York, 1993).